Hindawi
Journal of Spectroscopy
Volume 2018, Article ID 3480384, 14 pages
https://doi.org/10.1155/2018/3480384

Research Article

4-Hydroxycoumarin Derivative: *N*-(diphenylmethyl)-2-[(2-oxo-2H-chromen-4-yl)oxy]acetamide Interaction with Human Serum Albumin

Shanmugavel Chinnathambi,[1] **Subramani Karthikeyan**,[2] **Mangaiyarkarsi Rajendiran**,[2] **Kanniyappan Udayakumar**,[2] **Arunkumar Manoharan**,[3] **Saravanan Kandasamy**,[4] **and Nobutaka Hanagata**[5]

[1]*International Center for Young Scientists, National Institute for Materials Science, 1-2-1 Sengen, Tsukuba, Ibaraki 305-0047, Japan*
[2]*Department of Medical Physics, Anna University, Chennai 600025, India*
[3]*Centre for Nanoscience and Technology, Anna University, Chennai 600025, India*
[4]*Department of Physics, Periyar University, Salem 636011, India*
[5]*Nanotechnology Innovation Station, National Institute for Materials Science, 1-2-1 Sengen, Tsukuba, Ibaraki 305-0047, Japan*

Correspondence should be addressed to Shanmugavel Chinnathambi; chinnathambi.shanmugavel@nims.go.jp and Nobutaka Hanagata; hanagata.nobutaka@nims.go.jp

Received 13 April 2018; Revised 24 July 2018; Accepted 8 August 2018; Published 16 October 2018

Academic Editor: Wei Kong

In this study, the interaction between the coumarin derivative: *N*-(diphenylmethyl)-2-[(2-oxo-2*H*-chromen-4-yl)oxy]acetamide, biologically active drug, and human serum albumin (HSA) was investigated by using various optical spectroscopy techniques along with the computational technique. The results of steady-state fluorescence spectroscopy show that the static quenching occurred while increasing the coumarin drug concentration into HSA. Also, the binding constant (K) and thermodynamical parameters of enthalpy change (ΔH°), entropy change (ΔS°), and Gibbs free energy change (ΔG°) were calculated at different temperatures (293 K, 298 K, and 303 K). The results are in good agreement with those of molecular docking studies, and also, the docking study was carried out to understand the hydrogen bonding and hydrophobic interaction between human serum albumin and coumarin derivative. In addition to the docking, charge distribution analysis was done to understand the internal stability of coumarin derivative active sites of human serum albumin. Further time-resolved emission spectroscopy (TRES) studies were carried out between free HSA and HSA-coumarin complex, and the result confirms the presence of the drug in the protein molecule without cytotoxicity.

1. Introduction

Coumarin and its derivatives have been known for a long time, yet their vital role in plant and animal systems has not been thoroughly analyzed. Many coumarins and their derivatives exert antitumor, antiviral, anticoagulant, anti-inflammatory, antioxidant, vasorelaxant, antimicrobial, and enzyme inhibition properties. These compounds are precisely known to exert an antitumor effect and can cause significant changes in the regulation of the immune response, cell growth, and differentiation. Coumarins have recently attracted much attention due to their broad pharmacological activities as precursor molecules for the synthesis of some synthetic anticoagulant drugs [1–6]. Coumarin (2-oxo-2H-chromene) is a naturally occurring heterocyclic compound isolated from various plants; it has been found in the microorganisms, animals, essential oils, and fruits [4, 7–12]. *N*-(diphenylmethyl)-2-[(2-oxo-2H-chromen-4-yl)oxy]acetamide (Figure 1(b), already reported by Govindhan et al.) [13] which originates from

4-hydroxycoumarin shows the functional biological activity and also the more biologically active site of the coumarin family make more interest on, to understand the pharmacokinetic mechanism into the carrier molecule.

Serum albumins (Figure 1(a)) are the most fruitful proteins in the circulatory route of a wide diversity of various creatures and also blew the lid off the crucial first nature in the binding and transport of various endogenous and exogenous ligands. The molecular interactions of proteins and lots of compounds like medicine and a few organic molecules are investigated successfully. However, the binding of 4-hydroxycoumarin products to serum albumins is now an emerging field to explore the role, in biological systems, and their mode of action in various diseases [14].

In the present study, synthesized *N*-(diphenylmethyl)-2-[(2-oxo-2H-chromen-4-yl)oxy]acetamide interaction with human serum albumin was carried out using various optical spectroscopy techniques. Also, computational techniques like molecular docking and density functional theory (DFT) were performed further to understand the hydrogen bonding, hydrophobic information with active site residues, internal stability, and charge distribution of the molecule at the atomic level [15].

2. Experimental Section

2.1. Reagents. *N*-(diphenylmethyl)-2-[(2-oxo-2H-chromen-4-yl)oxy]acetamide is newly synthesized, which is already reported by Govindan et al. [13], and the same drug was dissolved in 0.5% DMSO in the PBS buffer. Human serum albumin was purchased from Sigma-Aldrich, USA, and used without any further purification.

2.2. Fluorescence Measurements. The emission spectroscopy study was performed using a spectrofluorometer (ISA FluoroMax-2; Jobin Yvon-Spex, Edison, NJ); the spectral bandpass was fixed at 5 nm for monochromators of both wavelengths of excitation and emission, and the recorded wavelength region is 300–500 nm at 280 nm excitation. The lifetime fluorescence measurements of the coumarin derivative and human serum albumin complex were detected using Fluorolog (Horiba Jobin Yvon IBH, UK) with a fast response sensitive PMT detector (Hamamatsu Photonics, Japan) for an excitation wavelength of 280 nm to 450 nm. The decays were sliced and normalized each wavelength for HSA and HSA-coumarin complex. The excitation-emission matrix (EEM) was mapped with the following two conditions: the emission wavelength was recorded between 200 and 700 nm and the initial excitation wavelength was set to 200 nm with an increment of 10 nm. In EEM measurements, the spectral bandpasses were kept at 5 nm for both excitation and emission. In addition to that, the Forster resonance energy transfer analysis between the donor and acceptor and further single-point polarization studies between human serum albumin and the coumarin derivative complex were also carried out.

2.3. FTIR and CD Spectroscopy Measurements. Fourier-transform infrared spectra (FTIR) of the human serum albumin solutions were administered at temperature by using an FTIR spectrometer (Interspec 2020; Estonia) in the attenuated total reflection (ATR) mode with a resolution of 4 cm^{-1} and 32 scans. The secondary structural analysis was carried out using circular dichroism (CD) for free human albumin and complex using a spectropolarimeter (Jasco J715; MD, USA) employing a quartz cell of 0.1 cm beam bath.

2.4. Docking Studies. The human serum albumin structure was taken from the Protein Data Bank (PDB ID: 4L8U), and the coumarin derivative is drawn using the ChemDraw software. Proteins and small molecules are energetically minimized using the OPLS 2005 force field (Schrödinger LLC) used for molecular docking [15].

2.5. DFT Methods. Energy minimization has been performed using the density functional theory (DFT) methodology with B3LYP functional and 6-311G∗∗ basis sets for both coumarin molecule and cofactor with active site amino acids of HSA using the Gaussian 03 software. The electrostatic potential countermaps were pictured using the GView software [16].

2.6. Cell Viability Studies. The cytotoxic assay for the drug was obtained using the Cell Counting Kit-8 (CCK-8) (Dojindo Laboratories, Osaka, Japan). The cell density in the 96-well plate was 5000 cells/well, 24 hours later; the drug was added to the culture plate and incubated for another 24 h. After drug exposure, the cells were incubated with 10 μL CCK-8 for 2 h, and the absorbance at 450 nm was measured using a microplate reader (MTP-880Lab; Corona, Hitachinaka, Japan). The cytotoxicity was represented as a percentage of untreated control cells.

3. Results and Discussion

3.1. Fluorescence Spectroscopy Studies. The steady-state fluorescence spectroscopy is the most effective technique to understand the further binding mechanism of the HSA-coumarin derivative complex. In general, the human serum albumin emission will be at 350 nm due to the presence of tryptophan residue and other phenylalanines; tyrosine residues emission is considered to be less compared to tryptophan residues emission. The emission spectrum of HSA (1 μM) and various concentrations of the coumarin derivative (0–3.6 μM) is shown in Figure 2(a), and it is indicated that there is a decrease without a shift in emission maximum of the HSA-coumarin derivative complex. Hence, we may conclude that fluorescence quenching occurs due to the presence of the coumarin derivative [17].

To know more about the type of quenching, we performed Stern–Volmer (Equation (1)) calculation at a different temperature as shown in Figure 2(b), and the calculated results of the quenching constant are tabulated in Table 1 [18, 19]:

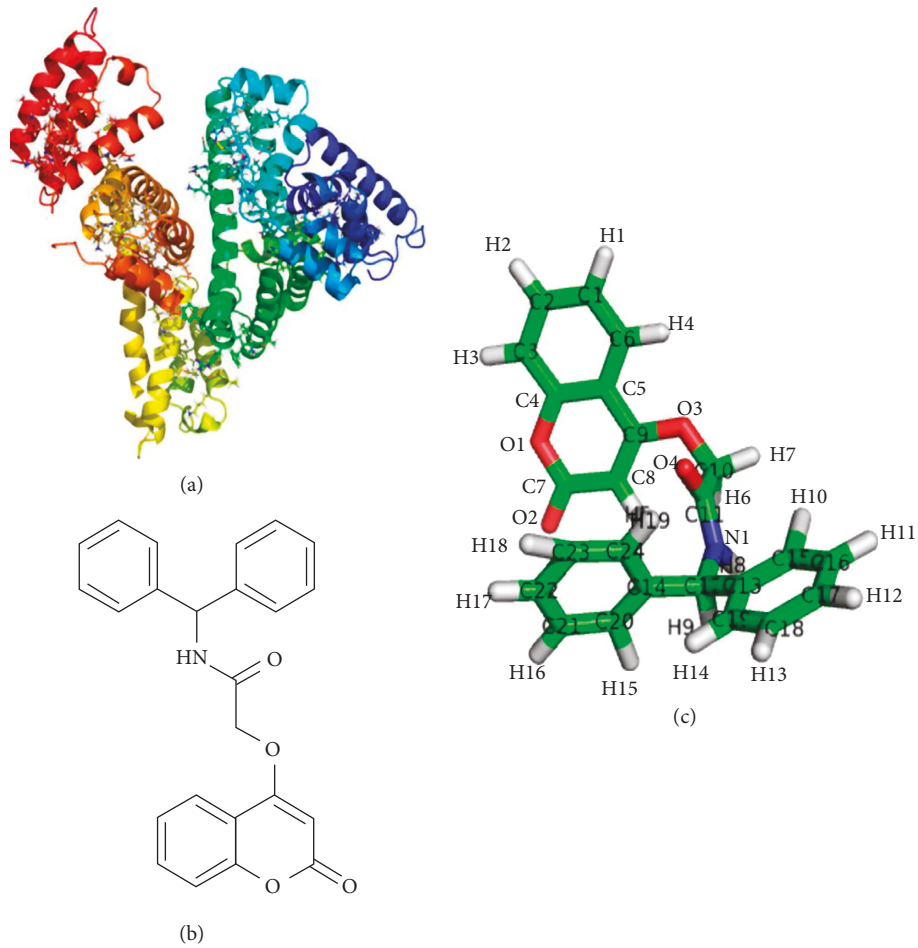

Figure 1: (a) Crystal structure of human serum albumin (PDB ID: 4L8U). (b) Chemical structure of the coumarin derivative. (c) Pymol view of the energy-minimized structure of the coumarin derivative.

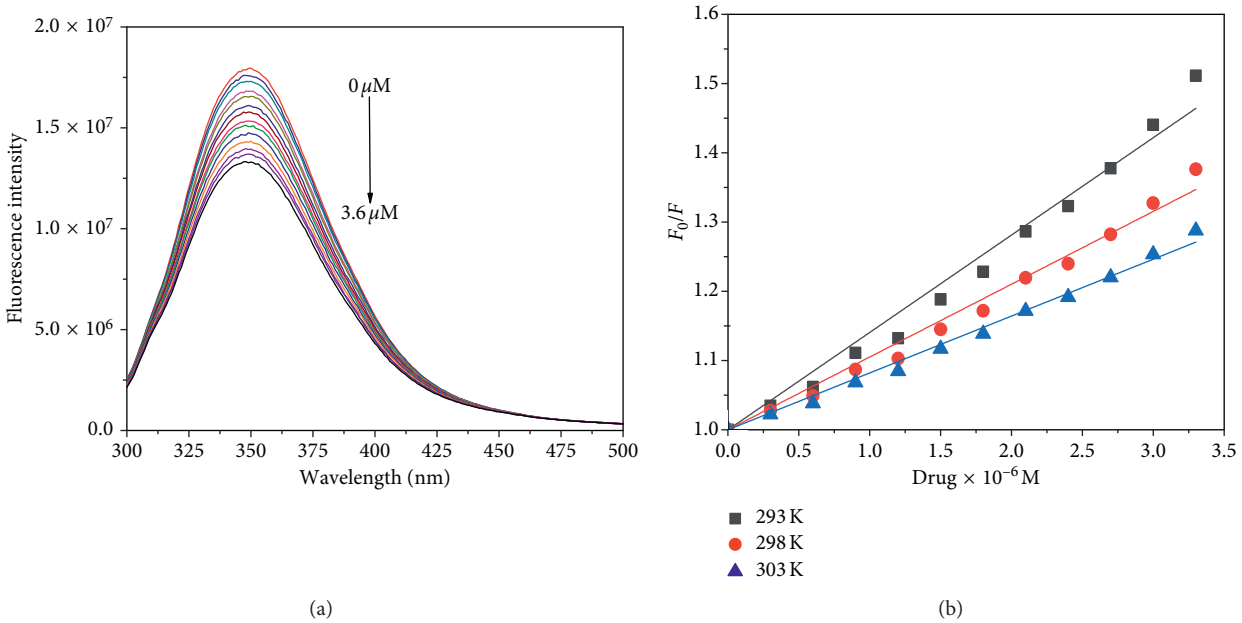

Figure 2: Continued.

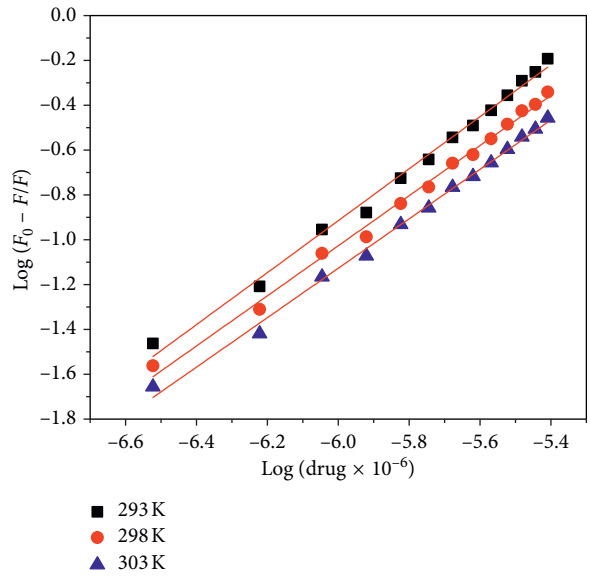

(c)

Figure 2: (a) Steady-state emission fluorescence spectroscopy studies of human serum albumin (1 μM) with the coumarin derivative complex (0–3.6 μM, 0.3 μM intervals). (b) The Stern–Volmer quenching constant of the HSA-coumarin derivative complex with different temperatures. (c) The double logarithmic plot of HSA with the coumarin derivative complex at different temperatures.

$$\frac{F_0}{F} = 1 + k_q \tau_0 [Q] = 1 + K_{SV} [Q], \quad (1)$$

where F_0 and F is the free HSA and HSA complex (coumarin drug), k_q is the bimolecular quenching constant ($k_q = K_{SV} \times \tau_0^{-1}$), τ_0 is the lifetime of the fluorophore without the drug molecule (10^{-8} s), K_{SV} is the Stern–Volmer quenching constant (0.79×10^{-5}, 1.00×10^{-5}, and 1.33×10^{-5} $mol^{-1} \cdot s^{-1} \cdot L^{-1}$), and $[Q]$ denotes the concentration of the drug. From Table 1, the calculation result of k_q indicates that static quenching occurs due to the complex formation of the coumarin derivative. The binding constant and number of binding sites were calculated using the following equation [20]:

$$\log \left[\frac{(F_0/F)}{F} \right] = \log [K_a] + n \log [Q], \quad (2)$$

where $[K_a]$ and $[Q]$ are the total concentration of HSA and coumarin drug, respectively, and the binding constant and number of binding sites were obtained and tabulated in Table 1 using the least-square fitting algorithm (Figure 2(c)).

3.2. Thermodynamic Parameter Analysis. The thermodynamic study is important for the drug-binding mechanism to calculate the binding stability of the drug with the macromolecule complex. Thermodynamics parameters ΔH°, ΔS°, and ΔG° are calculated from the following equations:

$$\log K_a = -\frac{\Delta H^\circ}{2.303RT} + \frac{\Delta S^\circ}{2.303R},$$
$$\Delta G^\circ = \Delta H^\circ - T\,\Delta S^\circ = -RT \ln K_a, \quad (3)$$

where R is the gas constant and T is the temperature, and here, three different temperatures are used: 293 K, 298 K, and 303 K.

According to Ross and Subramanian [17, 21, 22], the enthalpy change (ΔH°) and entropy change (ΔS°) tabulated in Table 1 indicate that ($\Delta H^\circ < 0$ and $\Delta S^\circ > 0$) type of interaction between HSA and the coumarin derivative complex is maybe due to the electrostatic interaction.

3.3. Time-Resolved Emission Spectroscopy Studies (TRES) and Fluorescence Lifetime Studies. Time-resolved emission spectroscopy is one of the highly noninvasive techniques to understand the real-time dynamics of biomolecules. Figure 3(a) shows the emission decay profile of free HSA and HSA-coumarin derivative complex; each point consists of average photons of respective wavelengths. All the recorded emission profiles of HSA and HSA complex followed the multiexponential decay kinetics, and the average lifetime decay for free HSA was found to be 4.83 ns which is almost equal to previously reported values [21, 23]. However, in the case of HSA-coumarin derivative complex, the decay is slightly faster compared to that of free HSA, and the average estimation of the HSA complex is 4.67 ns (Table 2). From Figure 3(b), the observed result indicates that quenching occurs due to the binding of the coumarin derivative with HSA. It is important to mention that the emission decay profile of the HSA complex is faster than that of free HSA in all wavelengths due to carrying of the coumarin derivative. This present result elucidates that protein unfolding is possible in the HSA complex because of the presence of the drug, and also, the tryptophan region gets more exposed to water. These results suggest that free HSA is more labile and

Table 1: Fluorescence binding parameters for HSA-coumarin derivatives (pH 7.4).

Compound	T (K)	k_q ($\times 10^{13}$ l·mol^{-1}·s^{-1})	K_b ($\times 10^5$ l/mol)	n	ΔH° (kJ/mol)	ΔG° (kJ/mol)	ΔS° (J/mol/K)
Coumarin derivatives	293	7.41	6.04	1.15	−10.35	−25.34	86.51
	298	5.82	5.67	1.11		−25.76	
	303	4.38	5.48	1.10		−26.19	

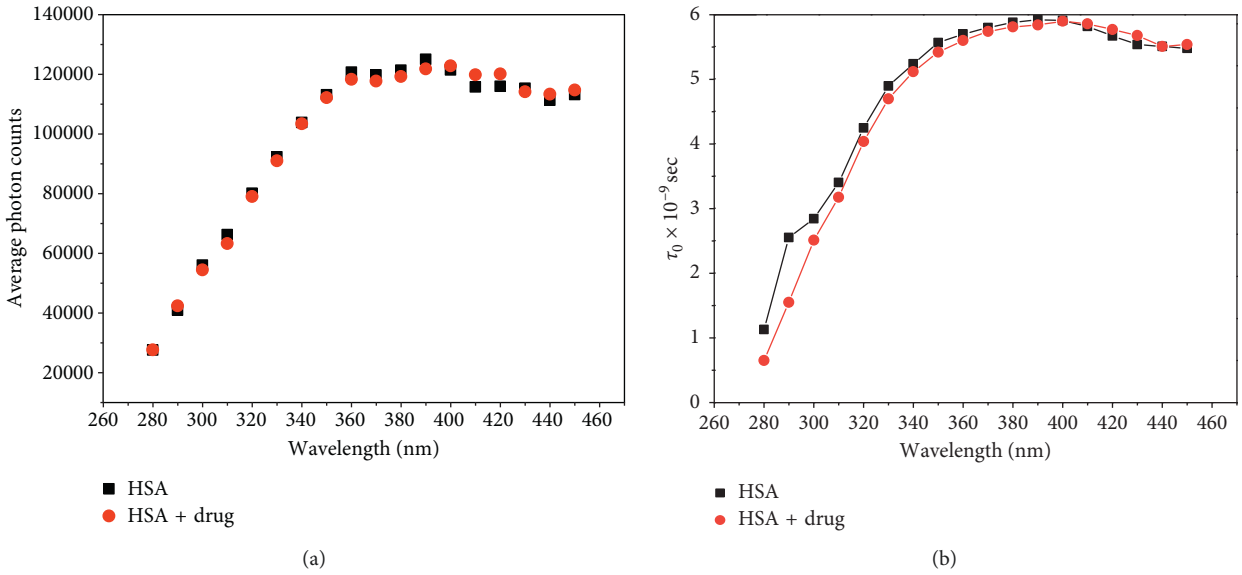

Figure 3: (a) Time-resolved emission spectroscopy (TRES) studies of HSA (1 μM) with the drug complex (1 μM) of different wavelength decay parameters. (b) Global fitted τ_0 value for each wavelength of the respective HSA and HSA-coumarin derivative.

Table 2: Fluorescence lifetime profiles of HSA and increasing concentration of coumarin derivatives at different excitation wavelengths.

Wavelength (nm)	$\alpha_1 \pm$ (error $\times 10^{-3}$)	$\alpha_2 \pm$ (error $\times 10^{-3}$)	$\alpha_3 \pm$ (error $\times 10^{-3}$)	τ_1 (ns)	τ_2 (ns)	τ_3 (ns)	$\tau_0 = (\sum_{i=1}^{i=3}\alpha_i\tau_i^2)/(\sum_{i=1}^{i=3}\alpha_i\tau_i)$ (ns)	χ^2
Fluorescence decay-fitting parameters for free HSA								
280	0.00098 ± 0.012	0.74 ± 5.13	0.00015 ± 0.02	2.12 ± 0.008	0.0097 ± 0.002	6.82 ± 0.006	1.13	0.5
290	0.017 ± 0.024	0.61 ± 5.60	0.00106 ± 0.05	2.12 ± 0.008	0.0097 ± 0.002	6.82 ± 0.006	2.55	1.03
300	0.037 ± 0.033	0.29 ± 5.34	0.0024 ± 0.07	2.12 ± 0.008	0.0097 ± 0.002	6.82 ± 0.006	2.84	1.42
310	0.037 ± 0.036	0.21 ± 5.13	0.0047 ± 0.086	2.12 ± 0.008	0.0097 ± 0.002	6.82 ± 0.006	3.40	1.19
320	0.037 ± 0.042	0.15 ± 5.31	0.010 ± 0.013	2.12 ± 0.008	0.0097 ± 0.002	6.82 ± 0.006	4.24	1.12
330	0.035 ± 0.046	0.093 ± 5.34	0.016 ± 0.013	2.12 ± 0.008	0.0097 ± 0.002	6.82 ± 0.006	4.89	1.09
340	0.032 ± 0.048	0.042 ± 5.24	0.020 ± 0.014	2.12 ± 0.008	0.0097 ± 0.002	6.82 ± 0.006	5.23	1.00
350	0.027 ± 0.05	0.027 ± 5.23	0.024 ± 0.015	2.12 ± 0.008	0.0097 ± 0.002	6.82 ± 0.006	5.56	1.00
360	0.026 ± 0.051	0.00054 ± 5.0	0.026 ± 0.016	2.12 ± 0.008	0.0097 ± 0.002	6.82 ± 0.006	5.69	1.05
370	0.024 ± 0.050	0.0018 ± 5.0	0.027 ± 0.016	2.12 ± 0.008	0.0097 ± 0.002	6.82 ± 0.006	5.79	0.96
380	0.023 ± 0.052	0.0061 ± 5.1	0.029 ± 0.016	2.12 ± 0.008	0.0097 ± 0.002	6.82 ± 0.006	5.87	1.00
390	0.022 ± 0.051	0.0031 ± 5.1	0.028 ± 0.016	2.12 ± 0.008	0.0097 ± 0.002	6.82 ± 0.006	5.91	0.91

Table 2: Continued.

Wavelength (nm)	$\alpha_1 \pm$ (error $\times 10^{-3}$)	$\alpha_2 \pm$ (error $\times 10^{-3}$)	$\alpha_3 \pm$ (error $\times 10^{-3}$)	τ_1 (ns)	τ_2 (ns)	τ_3 (ns)	$\tau_0 = (\sum_{i=1}^{i=3}\alpha_i\tau_i^2)/(\sum_{i=1}^{i=3}\alpha_i\tau_i)$ (ns)	χ^2
400	0.022 ± 0.051	0.016 ± 5.0	0.029 ± 0.016	2.12 ± 0.008	0.0097 ± 0.002	6.82 ± 0.006	5.90	1.00
410	0.024 ± 0.051	0.007 ± 5.0	0.027 ± 0.016	2.12 ± 0.008	0.0097 ± 0.002	6.82 ± 0.006	5.81	1.00
420	0.028 ± 0.051	0.035 ± 5.0	0.026 ± 0.016	2.12 ± 0.008	0.0097 ± 0.002	6.82 ± 0.006	5.66	1.00
430	0.029 ± 0.053	0.029 ± 4.9	0.024 ± 0.015	2.12 ± 0.008	0.0097 ± 0.002	6.82 ± 0.006	5.53	1.00
440	0.030 ± 0.050	0.030 ± 4.9	0.023 ± 0.015	2.12 ± 0.008	0.0097 ± 0.002	6.82 ± 0.006	5.50	1.00
450	0.031 ± 0.050	0.038 ± 4.9	0.023 ± 0.015	2.12 ± 0.008	0.0097 ± 0.002	6.82 ± 0.006	5.47	0.99
Fluorescence decay-fitting parameters for the HSA-coumarin derivative complex								
280	0.0015 ± 0.011	0.00004 ± 0.0013	0.815 ± 5.5	1.9 ± 0.0082	6.8 ± 0.0065	0.009 ± 0.002	0.65	0.34
290	0.0051 ± 0.016	0.00021 ± 0.0021	0.806 ± 5.9	1.9 ± 0.0082	6.8 ± 0.0065	0.009 ± 0.002	1.55	0.73
300	0.029 ± 0.030	0.0015 ± 0.0054	0.499 ± 6.0	1.9 ± 0.0082	6.8 ± 0.0065	0.009 ± 0.002	2.51	1.07
310	0.037 ± 0.037	0.0004 ± 0.0073	0.374 ± 6.1	1.9 ± 0.0082	6.8 ± 0.0065	0.009 ± 0.002	3.17	1.16
320	0.038 ± 0.042	0.0008 ± 0.0096	0.20 ± 5.9	1.9 ± 0.0082	6.8 ± 0.0065	0.009 ± 0.002	4.03	1.11
330	0.041 ± 0.049	0.015 ± 0.012	0.095 ± 5.9	1.9 ± 0.0082	6.8 ± 0.0065	0.009 ± 0.002	4.69	1.07
340	0.037 ± 0.050	0.019 ± 0.013	0.025 ± 5.6	1.9 ± 0.0082	6.8 ± 0.0065	0.009 ± 0.002	5.11	0.98
350	0.035 ± 0.053	0.024 ± 0.014	0.012 ± 5.6	1.9 ± 0.0082	6.8 ± 0.0065	0.009 ± 0.002	5.41	1.01
360	0.030 ± 0.053	0.025 ± 0.014	0.020 ± 5.4	1.9 ± 0.0082	6.8 ± 0.0065	0.009 ± 0.002	5.59	0.97
370	0.029 ± 0.055	0.029 ± 0.015	0.035 ± 5.5	1.9 ± 0.0082	6.8 ± 0.0065	0.009 ± 0.002	5.73	1.09
380	0.026 ± 0.054	0.029 ± 0.015	0.049 ± 5.3	1.9 ± 0.0082	6.8 ± 0.0065	0.009 ± 0.002	5.80	1.03
390	0.026 ± 0.055	0.030 ± 0.016	0.072 ± 5.2	1.9 ± 0.0082	6.8 ± 0.0065	0.009 ± 0.002	5.83	0.98
400	0.024 ± 0.054	0.029 ± 0.016	0.075 ± 5.0	1.9 ± 0.0082	6.8 ± 0.0065	0.009 ± 0.002	5.89	1.13
410	0.027 ± 0.055	0.031 ± 0.016	0.11 ± 5.0	1.9 ± 0.0082	6.8 ± 0.0065	0.009 ± 0.002	5.85	1.06
420	0.028 ± 0.054	0.028 ± 0.016	0.15 ± 4.7	1.9 ± 0.0082	6.8 ± 0.0065	0.009 ± 0.002	5.76	1.26
430	0.030 ± 0.054	0.027 ± 0.016	0.17 ± 4.5	1.9 ± 0.0082	6.8 ± 0.0065	0.009 ± 0.002	5.67	1.15
440	0.033 ± 0.054	0.026 ± 0.016	0.19 ± 4.4	1.9 ± 0.0082	6.8 ± 0.0065	0.009 ± 0.002	5.50	1.17
450	0.032 ± 0.053	0.025 ± 0.015	0.21 ± 4.2	1.9 ± 0.0082	6.8 ± 0.0065	0.009 ± 0.002	5.53	1.04

has faster hydration dynamics, and the similar process occurs in the HSA-coumarin derivative complex without any structural disturbance. Figure 3(b) represents the decay parameter-fitted values τ_0 of free HSA and HSA-coumarin derivative complex for easy understanding.

3.4. Excitation-Emission Matrix (EEM) Analysis. The study is used to further understand the conformational change of HSA more carefully during the interaction with the coumarin derivative. Figure 4 shows the contour map of free HSA (a) and coumarin derivative-HSA complex (b) with the corresponding characteristic parameters presented. There are two major fluorescence peaks observed in the figures: peak 1 and peak 2. Peak 1 (λ_{ex} = 220 nm and λ_{em} = 325 nm) is mainly due to polypeptide backbone structures, which correlated with the secondary structure of the protein, and peak 2 arises mainly (λ_{ex} = 278 nm and λ_{em} = 344 nm) due to

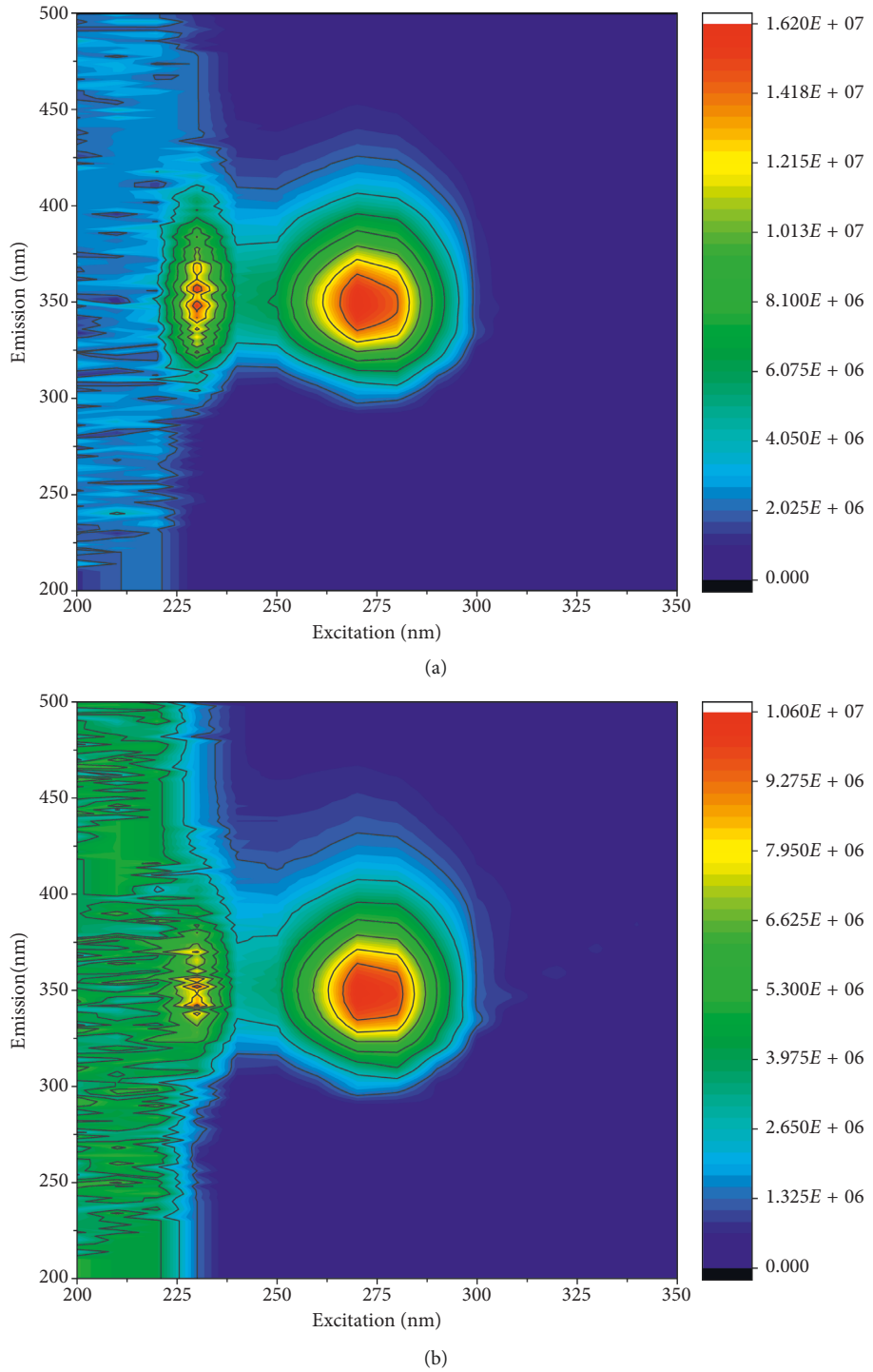

Figure 4: Excitation-emission matrix spectra of (a) free HSA (1 μM) and (b) HSA with the coumarin derivative complex (1 μM).

the presence of tryptophan and tyrosine residues. From Figure 4, it is observed that there is a decrease in intensity maxima while adding the coumarin derivative into free HSA, and the quenching in both peak 1 and peak 2 may be due to the presence of the coumarin derivative, suggesting that the compound may be nearby the HSA chromophore. These results conclude that there may be slight confirmation changes in HSA due to the presence of the coumarin derivative [23, 24].

3.5. FTIR Spectroscopy Studies. In general, the FTIR spectral technique is performed to understand the biochemical changes; here, the FTIR spectra of HSA were recorded to investigate the conformational changes to understand the binding mechanism of the coumarin derivative. Figure 5(a) shows the spectrum of free HSA and HSA-coumarin derivative complex, and the amide I peak of HSA is lying between 1600 and 1700 cm^{-1} and amide II region is almost in 1558 cm^{-1}, which is almost similar to the secondary

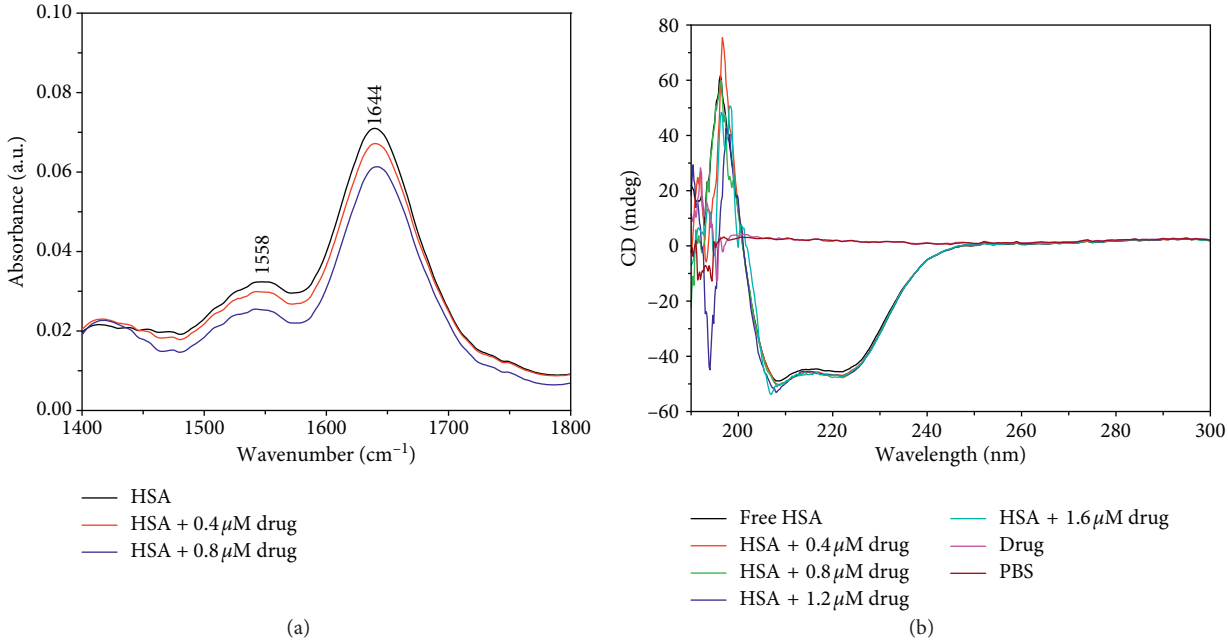

Figure 5: (a) FTIR spectra analysis of HSA (1 μM) and HSA-coumarin derivative complex (0–0.8 μM). (b) CD spectral analysis of HSA (1 μM) and HSA-coumarin derivative complex (0–1.4 μM).

Table 3: Binding energy and hydrogen bonding interaction of the coumarin derivative with HSA active site residues.

Compound name	Hydrogen bond (D-H...A)	Distance (Å)	Binding energy (kJ/mol)
Coumarin derivative	N–H···O (LEU 185)	3.0	−28.32
	N–H···O (ARG 117)	2.9	

structure of proteins. Comparing these two bands, amide I is strong (1644 cm^{-1}) as shown in Figure 5(a), and also while adding the coumarin derivative into free HSA, there is a decrease observed in the absorption of amide I maxima, which may be due to the coumarin derivative disturbance of the HSA amide region [21, 23, 24].

3.6. Circular Dichroism (CD) Spectral Analysis. To understand the conformational changes of the protein secondary structure, CD spectral analysis was carried out. From Figure 5(b), CD spectra of HSA show that there are two negative bands in the ultraviolet region, at 208 nm and 222 nm. When the coumarin derivative is added into the free HSA molecule, there are notable increases observed in both 208 and 222 nm intensities while increasing the concentration and also particularly at 208 nm region of HSA (1 μM) and HSA-coumarin derivative (1.6 μM) show a slight shift towards the lower wavelength region, indicating that the α-helical structure may lose stability or rearrange the orientation of total structural confirmation due to presence of the coumarin derivative.

Secondary structure calculations were carried out using the DichroWeb (http://dichroweb.cryst.bbk.ac.uk/html/home.shtml) online tool for the free HSA that consists of ~54.2% α-helix, ~22.1% β sheets, and 16.3% of the random coil, which are almost comparable with previously published data [17, 24].

For the coumarin derivative at 1.6 μM concentration, the secondary structure parameters increased with respect to ~58.1% α-helix, ~24.7% β sheets, and 19.2% of the random coil, respectively. These results show that the secondary structure of HSA may be partially unfolded or reorientation occurs in the overall structure due to the presence of the coumarin derivative.

3.7. Molecular Docking Studies. The molecular docking method is useful to understand the binding insight mechanism between the macromolecule and the small molecule at the atomic level [25, 26]. In this work, the molecular docking between HSA and coumarin derivative was performed using AutoDock 4.2 to clarify further the binding mode of coumarin derivative and HSA. Here, both small molecules and macromolecules are allowed for flexible docking, and the free energy values and hydrogen bonding and hydrophobic information results are shown in Table 3. Docking results show that the binding interaction between HSA and the coumarin derivative is in good agreement regarding energy and interaction. Figures 6(a) and 6(b) show the hydrogen bonding and hydrophobic information of the HSA-coumarin derivative complex further to understand more about internal stability of the coumarin derivative, and the charge distribution analysis was carried out at active residues of the HSA-coumarin derivative complex.

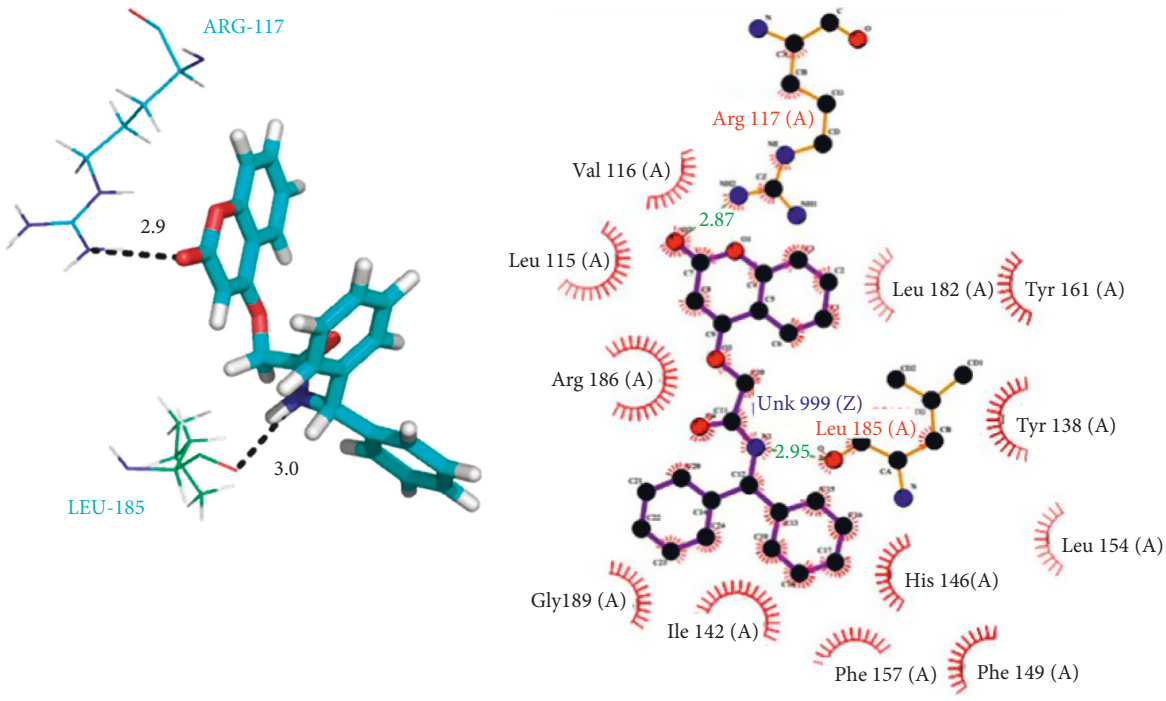

(a) (b)

Figure 6: (a) Pymol view of HSA-coumarin derivative complex hydrogen bonding interaction with active site residues. (b) Charge distribution (DFT) analysis plot for the HSA-coumarin derivative complex of active site residues.

Table 4: The calculated Mulliken population analysis (MPA) of the coumarin molecule with active site amino acids of HSA.

MPA			MPA cofactor		
1N −0.38	51C −0.06	101C −0.06	1N −0.43	51O −0.28	101C 0.06
2C −0.05	52C −0.05	102C 0.32	2C −0.11	52C −0.18	102C −0.16
3C 0.16	53C −0.13	103C 0.08	3C 0.15	53C −0.09	103C 0.14
4O −0.24	54C −0.09	104C −0.10	4O −0.30	54C −0.05	104C 0.29
5C −0.20	55C 0.12	105C −0.14	5C −0.16	55C −0.05	105N −0.38
6C −0.27	56O −0.38	106C −0.03	6C −0.26	56C −0.09	106C 0.09
7C −0.09	57H 0.18	107C −0.09	7C −0.09	57C −0.06	107C −0.09
8N −0.44	58H 0.20	108C −0.09	8N −0.46	58C 0.12	108C 0.02
9C 0.68	59H 0.12	109C −0.09	9C 0.65	59O −0.41	109C −0.21
10N −0.45	60H 0.12	110C −0.06	10N −0.47	60H 0.25	110C 0.44
11N −0.46	61H 0.09	111C −0.07	11N −0.49	61H 0.19	111O −0.41
12H 0.15	62H 0.08	112C −0.09	12H 0.23	62H 0.12	112C 0.01
13H 0.10	63H 0.15	113C −0.09	13H 0.19	63H 0.08	113C 0.04
14H 0.09	64H 0.09	114C −0.10	14H 0.13	64H 0.12	114C 0.39
15H 0.11	65H 0.26	115C 0.00	15H 0.09	65H 0.08	115O −0.49
16H 0.14	66N −0.38	116H 0.11	16H 0.10	66H 0.08	116O −0.49
17H 0.12	67C −0.08	117H 0.12	17H 0.13	67H 0.10	117O −0.37
18H 0.14	68C 0.23	118H 0.17	18H 0.12	68H 0.08	118C −0.21
19H 0.14	69O −0.16	119H 0.11	19H 0.32	69H 0.10	119C −0.26
20H 0.27	70C −0.22	120H 0.13	20H 0.28	70H 0.19	120O −0.37
21H 0.25	71C −0.12	121H 0.13	21H 0.25	71N −0.45	121N −0.52
22H 0.26	72C −0.03	122H 0.15	22H 0.20	72C −0.07	122H 0.21
23H 0.24	73C −0.04	123H 0.26	23H 0.15	73C 0.19	123H 0.08
24H 0.28	74C −0.13	124H 0.15	24H 0.11	74O −0.28	124H 0.09
25N −0.49	75C −0.12	125H 0.07	25H 0.11	75C −0.21	125H 0.08
26C −0.05	76C 0.16	126H 0.09	26H 0.21	76C −0.06	126H 0.07
27C 0.03	77O −0.37	127H 0.09	27N −0.43	77C −0.04	127H 0.12
28O −0.30	78H 0.18	128H 0.09	28C −0.11	78C −0.07	128H 0.10
29C −0.24	79H 0.19	129H 0.10	29C 0.22	79C −0.12	129H 0.15

Table 4: Continued.

MPA			MPA cofactor		
30C −0.20	80H 0.15	130H 0.08	30O −0.29	80C −0.08	130H 0.23
31C −0.27	81H 0.12	131H 0.09	31C −0.22	81C 0.13	131H 0.11
32C −0.26	82H 0.08	132H 0.09	32C −0.20	82O −0.37	132H 0.10
33H 0.16	83H 0.08	133H 0.09	33C −0.25	83H 0.24	133H 0.22
34H 0.14	84H 0.09	134H 0.11	34C −0.26	84H 0.19	134H 0.22
35H 0.10	85H 0.12		35H 0.10	85H 0.12	135H 0.08
36H 0.09	86H 0.25		36H 0.20	86H 0.07	136H 0.11
37H 0.11	87C −0.09		37H 0.13	87H 0.11	137H 0.09
38H 0.10	88N −0.42		38H 0.08	88H 0.07	138H 0.10
39H 0.09	89O −0.31		39H 0.12	89H 0.08	
40H 0.10	90C −0.08		40H 0.09	90H 0.09	
41H 0.10	91O −0.39		41H 0.11	91H 0.12	
42H 0.10	92C −0.10		42H 0.10	92H 0.14	
43H 0.10	93O −0.35		43H 0.18	93H 0.19	
45N −0.39	94C 0.18		44H 0.11	94C −0.07	
46C −0.08	95O −0.37		45H 0.10	95C −0.08	
47C 0.24	96C −0.19		46H 0.10	96C −0.06	
48O −0.16	97C 0.00		47H 0.10	97C 0.10	
49C −0.20	98C 0.39		48N −0.44	98C −0.15	
50C −0.15	99C −0.25		49C −0.06	99C 0.20	
	100C 0.36		50C 0.19	100N −0.39	

3.8. Charge Distribution Analysis. The Mulliken atomic charges were analyzed for both coumarin derivative and cofactor with interaction amino acids of HSA. The MPA charges are presented in Table 4 (Figure 1(c)). The nitrogen atoms N_8, N_{10}, and N_{11} in the amino acid arginine possess high negative charges; simultaneously, the oxygen atoms O_{48} and O_{56} possess low negative charges. Because of these nitrogen atoms, interaction occurs with O_{48} and O_{56} atoms (N_8: −0.44e, N_{10}: −0.45e, N_{11}: −0.46e, O_{48}: −0.16e, and O_{56}: −0.38e), respectively; these charges are low compared with those in the cofactor. The oxygen atom O_{69} in tyrosine has a very low negative charge, which interacts with O_{91}. At the same time, the ligand contains nitrogen atom N_{45}, which also has a low negative charge (N_{45}: −0.39e, O_{69}: −0.16e, and O_{91}: −0.30e). From this, the MPA charges decreased while increasing the distance between the protein and ligand. The carbon C_9 atom possesses a high positive charge due to the carbon atom surrounded by nitrogen atoms [27].

The global reactivity descriptors [28–34] of the coumarin derivative and cofactor molecule such as electronegativity, electrophilicity, and chemical hardness have been calculated from HOMO and LUMO energies. The calculated values of ionization potential, electronegativity, and electron affinity of those molecules are 6.5/7.2, 8.1/9.6, and 1.6/2.4 eV (Table 5), and these values show that the coumarin derivative molecule has high tendency to accept electrons than the cofactor. The calculated electrophilicity of both molecules is 6.8/9.6 eV; this low value indicates that the molecule has low toxicity [35]. The chemical hardness of the molecule is 4.85/4.82 eV, which reveals that the molecule exhibits high kinetic stability and reactivity [16, 36–38]. The energy gap between the molecular orbitals is also calculated, and the HLG value is 4.86/4.82 eV, which indicates that both molecules have high internal stability. Figure 7 shows the electrostatic potential countermap of the coumarin derivative and cofactor with active site amino acids of HSA.

3.9. Steady-State Fluorescence Anisotropy Studies. Fluorescence anisotropy is widely used to measure the binding constants and kinetics of reactions that cause a change in the rotational time of the fluorescent molecules [24]. This technique will give information about changing the orientation of our coumarin derivative in human serum albumin. Here, the fluorescence anisotropy measurements were carried out between human serum albumin and a coumarin derivative of concentration ranging from 0 to 100 μM. Most reports say that anisotropy of small molecules may be zero and there is no rotation when it increases to the maximum value of 0.4. From Figure 8, coumarin derivative versus various increasing concentrations of human serum albumin shows that the anisotropy value of the coumarin derivative increases up to 20 μM and then reaches the steady-state maximum value (r = 0.13) after 40 μM of the HSA environment. This saturated value may be due to the coumarin derivative restriction in rotation motion of the HSA molecule, which also may be due to the formation of a hydrogen bond and hydrophobic interaction in active sites of HSA with the coumarin derivative.

3.10. Fluorescence Resonance Energy Transfer. The Forster energy transfer method is used to understand the energy distance between the donor and acceptor of biomolecules. The overlap absorbance spectrum of the drug and emission spectrum of human serum albumin are shown in Figure 9. The energy transfer efficiency (E) is used to calculate the distance between the coumarin derivative and human serum albumin. The rate of energy transfer depends on the integral overlap (J) of the donor (HSA) and acceptor (a coumarin derivative). Transition dipoles and distance between the drug and protein molecules also play a role in deciding the rate of energy transfer [17, 24]. The distance from the tryptophan residue which is located in the donor (HSA) and

Table 5: The calculated global reactivity properties of the coumarin derivative molecule.

Global reactivity descriptors	DFT (SP) of the coumarin derivative Active site Energy (eV)	DFT (SP) of the cocrystal drug Active site Energy (eV)
Band gap of LUMO-HOMO	4.857	4.825
HOMO energy	−6.501	−7.245
LUMO energy	−1.644	−2.422
Ionization potential $I = -E_{HOMO}$	6.501	7.245
Electron affinity $A = -E_{LUMO}$	1.644	2.422
Global hardness $\eta = (I - A)/2$	4.857	4.823
Electrophilicity $\omega = \mu^2/2\eta$	6.829	9.688
Electronegativity $X = I + A/2$	8.145	9.667

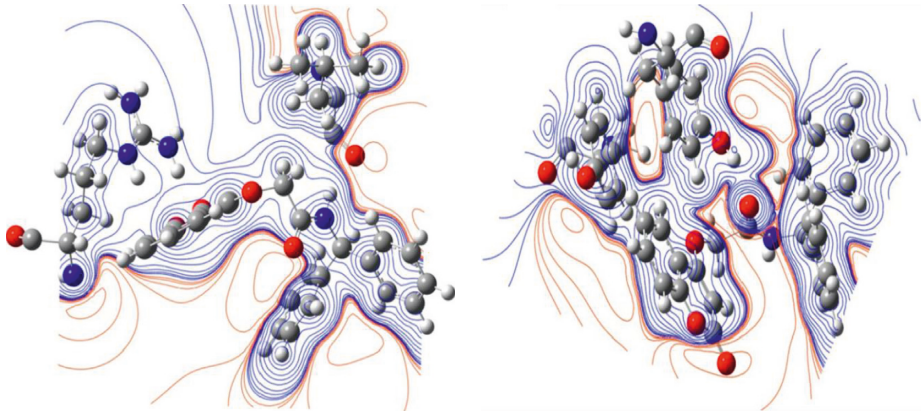

(a) (b)

Figure 7: The electrostatic potential countermap of the (a) coumarin derivative and (b) cofactor molecules with active site amino acids of HSA.

bound drug acceptor (a coumarin derivative) in HSA can be calculated using Forster's theory.

The energy transfer efficiency (E) was calculated using the following equation [39]:

$$E = 1 - \frac{F}{F_0} = \frac{R_0^6}{R_0^6 + r^6}, \quad (4)$$

where r is the distance between the donor and acceptor and R_0 is the critical distance between the donor and acceptor when their transfer efficiency is 50%:

$$R_0^6 = 8.79 \times 10^{-25}\left[k^2 n^{-4} \varphi_D J\right], \quad (5)$$

where k^2 is the orientation factor of the dipole, φ_D is the fluorescence quantum yield of the donor in the absence of the acceptor, and n is the refractive index of the complex medium:

$$J(\lambda) = \int_0^\infty F_D(\lambda)\varepsilon_A(\lambda)\lambda^4 \, d\lambda. \quad (6)$$

J is the integral overlap of the emission spectrum of the HSA (donor) with the absorption spectrum of the coumarin derivative (acceptor). $F_D(\lambda)$ is the fluorescence intensity of the donor at wavelength λ to $\lambda + \Delta\lambda$, with the total intensity normalized to unity, and $\varepsilon_A(\lambda)$ is the molar extinction coefficient of the acceptor at the wavelength (λ). It is possible for us to calculate the J value from the spectrum in which it is estimated that $J = 1.3182 \times 10^{-20}\,M^{-1}\cdot cm^3$. Under the experimental conditions, we have found $R_0 = 2.5$ nm from Equation (5). Using the following values, $E = 0.018$, $k^2 = 2/3$, $N = 1.336$ and $\phi_D = 0.118$, $r = 4.88$ nm has been calculated. Both R_0 and r values were found to be lower than the maximum values of R_0 (<10 nm), and the distance (r) between the donor and acceptor lies <7 nm.

3.11. Cytotoxicity of the Coumarin Derivative. The cytotoxicity of a coumarin derivative, which was used to evaluate its biocompatibility, was studied using the HeLa cell as a model cell by the CCK-8. Figure 10 shows the cell viability test results conducted for the coumarin derivative up to 30 μg/mL. As shown in Figure 10, the amount of the coumarin derivative increases and the cell viability decreases in a tiny percentage even at the maximum level of concentration at 30 μg/mL. However, coumarin derivative is a safe molecule to bind with the serum albumin protein and deliver the targeted tissue region.

4. Conclusion

In this context, the synthesized coumarin derivative molecules have been subjected to various spectroscopy and computational techniques for understanding the interaction mechanism in the HSA molecule. From the UV-Vis

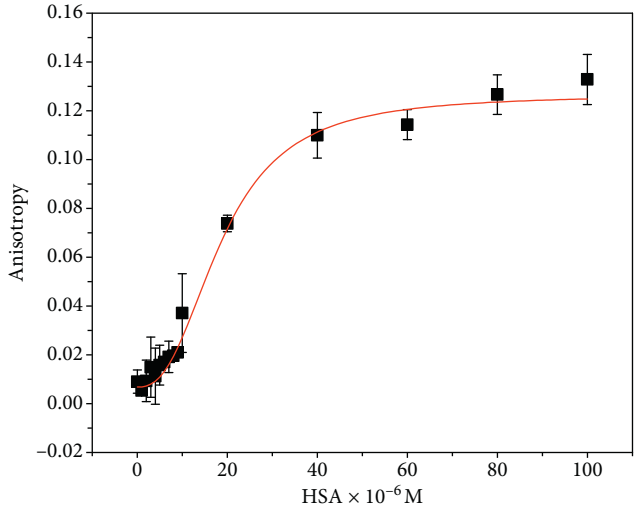

Figure 8: Anisotropy studies of the coumarin derivative with the HSA complex.

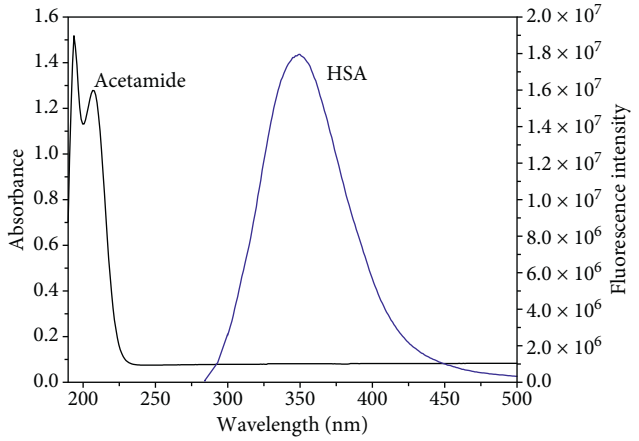

Figure 9: The distance between HSA and coumarin derivative.

absorbance result, it can be seen that the HSA-coumarin derivative complex may be due to the ground state complex; further fluorescence technique reveals that the coumarin derivative in the HSA complex is in the static quenching mode, and also, the thermal parameters calculated show good binding results. Time-resolved emission spectroscopy results show that the HSA molecule could be able to carry the coumarin derivative, and the calculated average lifetime value found for free HSA is 4.83 ns and for the HSA-coumarin derivative complex is 4.67 ns. Energy transfer analysis also calculated between donor and acceptor and r values is found that 4.88 nm, which is in academic value. The anisotropy results conclude that the rotation motion of HSA is saturated at $r = 0.13$ after the concentration of HSA 40 μM which is maybe due to the presence of the coumarin derivative. The excitation-emission matrix results suggest that the confirmation of HSA changed due to the presence of the coumarin derivative, and following this, the FTIR and CD spectral analysis also confirmed those secondary structure changes. Computational analysis elucidate the interaction

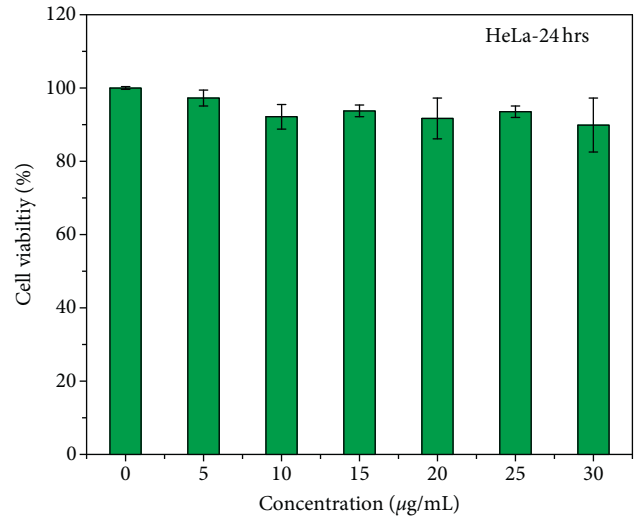

Figure 10: Cytotoxicity studies of the coumarin derivative.

mechanism of the HSA-coumarin derivative complex at the atomic level and information on bonding and internal stability; from this overall result, the binding nature of coumarin derivatives with HSA is good, and it could carry the molecule to a particular target without cytotoxicity.

Data Availability

The data used to support the findings of this study are available from the corresponding author upon request.

Conflicts of Interest

The authors declare that they have no conflicts of interest.

References

[1] T. Ojala, *Biological Screening of Plant Coumarins*, University of Helsinki, Helsinki, Finland, 2001.

[2] G. J. Finn, E. Kenealy, B. S. Creaven, and D. A. Egan, "In vitro cytotoxic potential and mechanism of action of selected coumarins using human renal cell lines," *Cancer Letters*, vol. 183, no. 1, pp. 61–68, 2002.

[3] D. A. Egan and R. O'Kennedy, "Rapid and sensitive determination of coumarin and 7-hydroxycoumarin and its glucuronide conjugate in urine and plasma by high-performance liquid chromatography," *Journal of Chromatography B: Biomedical Sciences and Applications*, vol. 582, no. 1-2, pp. 137–143, 1992.

[4] D. Egan, R. O'kennedy, E. Moran, D. Cox, E. Prosser, and R. D. Thornes, "The pharmacology, metabolism, analysis, and applications of coumarin and coumarin-related compounds," *Drug Metabolism Reviews*, vol. 22, no. 5, pp. 503–529, 1990.

[5] G. Keating and R. O'kennedy, *The Chemistry and Occurrence of Coumarins. Coumarins: Biology, Applications and Mode of Action*, p. 348, John Wiley & Sons Inc., New York, NY, USA, 1997.

[6] M. Riveiro, N. De Kimpe, A. Moglioni et al., "Coumarins: old compounds with novel promising therapeutic perspectives," *Current Medicinal Chemistry*, vol. 17, no. 13, pp. 1325–1338, 2010.

[7] A. Lacy and R. O'Kennedy, "Studies on coumarins and coumarin-related compounds to determine their therapeutic role in the treatment of cancer," *Current Pharmaceutical Design*, vol. 10, no. 30, pp. 3797–3811, 2004.

[8] C. Kontogiorgis and D. Hadjipavlou-Litina, "Biological evaluation of several coumarin derivatives designed as possible anti-inflammatory/antioxidant agents," *Journal of Enzyme Inhibition and Medicinal Chemistry*, vol. 18, no. 1, pp. 63–69, 2003.

[9] M. Campos-Toimil, F. Orallo, L. Santana, and E. Uriarte, "Synthesis and vasorelaxant activity of new coumarin and furocoumarin derivatives," *Bioorganic and Medicinal Chemistry Letters*, vol. 12, no. 5, pp. 783–786, 2002.

[10] L. M. Kabeya, A. A. Marchi, A. Kanashiro et al., "Inhibition of horseradish peroxidase catalytic activity by new 3-phenylcoumarin derivatives: synthesis and structure-activity relationships," *Bioorganic and Medicinal Chemistry*, vol. 15, no. 3, pp. 1516–1524, 2007.

[11] A. Chilin, R. Battistutta, A. Bortolato et al., "Coumarin as attractive casein kinase 2 (CK2) inhibitor scaffold: an integrated approach to elucidate the putative binding motif and explain structure-activity relationships," *Journal of Medicinal Chemistry*, vol. 51, no. 4, pp. 752–759, 2008.

[12] F. Borges, F. Roleira, N. Milhazes, L. Santana, and E. Uriarte, "Simple coumarins and analogues in medicinal chemistry: occurrence, synthesis and biological activity," *Current Medicinal Chemistry*, vol. 12, no. 8, pp. 887–916, 2005.

[13] M. Govindhan, K. Subramanian, K. Chennakesava Rao, K. Easwaramoorthi, P. Senthilkumar, and P. T. Perumal, "Synthesis of novel 4-hydroxycoumarin derivatives: evaluation of antimicrobial, antioxidant activities and its molecular docking studies," *Medicinal Chemistry Research*, vol. 24, no. 12, pp. 4181–4190, 2015.

[14] S. Chinnathambi, S. Karthikeyan, D. Velmurugan, N. Hanagata, P. Aruna, and S. Ganesan, "Effect of moderate UVC irradiation on bovine serum albumin and complex with antimetabolite 5-fluorouracil: fluorescence spectroscopic and molecular modelling studies," *International Journal of Spectroscopy*, vol. 2015, Article ID 315764, 12 pages, 2015.

[15] Schrödinger, LLC, *Biologics Suite 2009*, Schrödinger, LLC, New York, NY, USA, 2009.

[16] T. K. Roy Dennington and J. M. GaussView, *Version 5*, Semichem Inc., Shawnee Mission, KS, USA, 2009.

[17] S. Karthikeyan, G. Bharanidharan, K. A. Mani et al., "Determination on the binding of thiadiazole derivative to human serum albumin: a spectroscopy and computational approach," *Journal of Biomolecular Structure and Dynamics*, vol. 35, pp. 817–828, 2017.

[18] R. Mangaiyarkarasi, S. Chinnathambi, P. Aruna, and S. Ganesan, "Synthesis of 5-fluorouracil conjugated LaF_3:Tb^{3+}/PEGCOOH nanoparticles and its studies on the interaction with bovine serum albumin: spectroscopic approach," *Journal of Nanoparticle Research*, vol. 17, no. 3, p. 136, 2015.

[19] R. Mangaiyarkarasi, S. Chinnathambi, S. Karthikeyan, P. Aruna, and S. Ganesan, "Paclitaxel conjugated Fe_3O_4@ LaF_3:Ce^{3+},Tb^{3+} nanoparticles as bifunctional targeting carriers for cancer theranostics application," *Journal of Magnetism and Magnetic Materials*, vol. 399, pp. 207–215, 2016.

[20] X. Z. Feng, Z. Lin, L. J. Yang, C. Wang, and C. L. Bai, "Investigation of the interaction between acridine orange and bovine serum albumin," *Talanta*, vol. 47, no. 5, pp. 1223–1229, 1998.

[21] S. Karthikeyan, G. Bharanidharan, K. A. Mani et al., "Insights into the binding of thiosemicarbazone derivatives with human serum albumin: spectroscopy and molecular modelling studies," *Journal of Biomolecular Structure and Dynamics*, vol. 34, no. 6, pp. 1264–1281, 2016.

[22] P. D. Ross and S. Subramanian, "Thermodynamics of protein association reactions: forces contributing to stability," *Biochemistry*, vol. 20, no. 11, pp. 3096–3102, 1981.

[23] S. Chinnathambi, S. Karthikeyan, M. Kesherwani, D. Velmurugan, and N. Hanagata, "Underlying the mechanism of 5-fluorouracil and human serum albumin interaction: a biophysical study," *Journal of Physical Chemistry and Biophysics*, vol. 6, no. 2, pp. 2161–0398, 2016.

[24] S. Chinnathambi, D. Velmurugan, N. Hanagata, P. Aruna, and S. Ganesan, "Investigations on the interactions of 5-fluorouracil with bovine serum albumin: optical spectroscopic and molecular modeling studies," *Journal of Luminescence*, vol. 151, pp. 1–10, 2014.

[25] S. Karthikeyan, S. Chinnathambi, A. Kannan et al., "Investigation of optical spectroscopic and computational binding mode of bovine serum albumin with 1,4-bis ((4-((4-heptylpiperazin-1-yl) Methyl)-1H-1,2,3-triazol-1-yl) methyl) benzene," *Journal of Biochemical and Molecular Toxicology*, vol. 29, no. 8, pp. 373–381, 2015.

[26] S. Karthikeyan, S. Chinnathambi, D. Velmurugan, G. Bharanidharan, and S. Ganesan, "Insights into the binding of 3-(1-phenylsulfonyl-2-methylindol-3-ylcarbonyl) propanoic acid to bovine serum albumin: spectroscopy and molecular modelling studies," *Nano Biomedicine and Engineering*, vol. 7, no. 1, pp. 1–7, 2015.

[27] R. S. Mulliken, "Electronic population analysis on LCAO-MO molecular wave function," *Journal of Chemical Physics*, vol. 23, no. 10, pp. 1833–1840, 1955.

[28] U. Sarkar, D. R. Roy, P. K. Chattaraj, R. Parthasarathi, J. Padmanabhan, and V. Subramanian, "A conceptual DFT approach towards analyzing toxicity," *Journal of Chemical Sciences*, vol. 117, no. 5, pp. 599–612, 2005.

[29] D. R. Roy, U. P. Sarkar, K. Chattaraj et al., "Analyzing toxicity through electrophilicity," *Molecular Diversity*, vol. 10, no. 2, pp. 119–131, 2006.

[30] R. G. Parr, L. V. Szentpaly, and S. Liu, "Electrophilicity index," *Journal of the American Chemical Society*, vol. 121, pp. 1922–1924, 1999.

[31] R. G. Parr and R. G. Pearson, "Absolute hardness: companion parameter to absolute electronegativity," *Journal of the American Chemical Society*, vol. 105, no. 26, pp. 7512–7516, 1983.

[32] P. Geerlings, F. D. Proft, and W. Langencker, "Conceptual density functional theory," *Chemical Reviews*, vol. 103, no. 5, pp. 1793–1873, 2003.

[33] D. R. Roy, R. Parthasarathi, B. Maiti, V. Subramanian, and P. K. Chattaraj, "Electrophilicity as a possible descriptor for toxicity prediction," *Bioorganic and Medicinal Chemistry*, vol. 13, no. 10, pp. 3405–3412, 2005.

[34] K. Fukui, "Role of frontier orbitals in chemical reactions," *Science*, vol. 218, no. 4574, pp. 747–754, 1982.

[35] U. Sarkar, J. Padmanabhan, R. Parthasarathi, V. Subramanian, and P. K. Chattaraj, "Toxicity analysis of polychlorinated dibenzofurans through global and local electrophilicities," *Journal of Molecular Structure: THEOCHEM*, vol. 758, no. 2-3, pp. 119–125, 2006.

[36] M. Elango, R. Parthasarathi, V. Subramanian, U. Sarkar, and P. K. Chattaraj, "Formaldehyde decomposition through profiles of global reactivity indices," *Journal of Molecular Structure: THEOCHEM*, vol. 723, no. 1-3, pp. 43–52, 2005.

[37] P. K. Chattaraj, U. Sarkar, R. Parthasarathi, and V. Subramanian, "DFT study of some aliphatic amines using generalized philicity concept," *International Journal of Quantum Chemistry*, vol. 101, no. 6, pp. 690–702, 2004.

[38] P. K. Chattaraj, U. Sarkar, D. R. Roy, M. Elango, R. Parthasarathi, and V. Subramanian, "Is electrophilicity a kinetic or a thermodynamic concept?," *Indian Journal of Chemistry*, vol. 45A, pp. 1099–1112, 2006.

[39] S. Chinnathambi, N. Abu, and N. Hanagata, "Biocompatible CdSe/ZnS quantum dot micelles for long-term cell imaging without alteration to the native structure of the blood plasma protein human serum albumin," *RSC Advances*, vol. 7, no. 5, pp. 2392–2402, 2017.